Studying the impact of urban design on pollution flow

Environmental transport phenomena project
Fainello F., Mossinelli G., Venturi F.

Abstract

The goal of this project is to study the wind flow in a simple 2D model of a city. The main focus will be on the presence of a point source of pollutant upstream of the buildings, studying how the the reciprocal position of these affects the pollution of the front facades. This simple model will allow us to draw conclusions on how this analysis can help improve life quality in cities.

1 Introduction to the problem

The atmospheric boundary layer and its behaviour are strongly influenced by the roughness of the surface in contact with the fluid and the presence of objects of non-negligible size on it. A case of particular relevance is that of urban agglomerations. The interaction of the flow with buildings influences numerous aspects of daily life in and around cities, such as air traffic, wind intensity and the spread of pollutants. The layout of a city can be defined as a result of studying these phenomena in order to reduce the associated problems. In particular, the layout of buildings can affect the concentration of wind-borne pollutants within cities.

The issue discussed in the following concerns the way in which the reciprocal position of buildings leads to a possible reduction of pollution in internal and sensitive areas. Let us consider a two-dimensional case in which there is a point source of pollutant upstream of a complex consisting of two buildings. The pollutant considered is carbon monoxide (CO), transported by wind and diffused in dry air (composition $N_2 \sim 78\%, O_2 \sim 21\%, CO_2 \sim 0.04\%$) at $27°C$. Notice that the density of CO ($1.14 kg/m^3$) is sufficiently close to that of air ($1.17 kg/m^3$) in this scenario to neglect buoyancy.

2 Model

The analytical model governing the diffusion and transport of a fluid is represented by the well-known Navier-Stokes equations. The study of the above problem is carried out through the lateral view of a surface on which one or two buildings are constructed, depending on the simulations performed during the following study. For this reason, the mathematical model is reduced to the 2D version of the Navier-Stokes equations, which take the form:

$$
\begin{cases}
\dfrac{\partial u}{\partial x} + \dfrac{\partial v}{\partial y} = 0 \\
u\dfrac{\partial u}{\partial x} + v\dfrac{\partial u}{\partial y} = -\dfrac{1}{\rho}\dfrac{\partial p}{\partial x} + \mu\left(\dfrac{\partial^2 u}{\partial x^2} + \dfrac{\partial^2 u}{\partial y^2}\right) \\
u\dfrac{\partial v}{\partial x} + v\dfrac{\partial v}{\partial y} = -\dfrac{1}{\rho}\dfrac{\partial p}{\partial y} + \mu\left(\dfrac{\partial^2 v}{\partial x^2} + \dfrac{\partial^2 v}{\partial y^2}\right)
\end{cases}
\tag{1}
$$

where u is the velocity along the horizontal axis, v along the vertical one, p the pressure, ρ the density of the fluid and μ its kinematic viscosity.

Furthermore, the interest of the study lies in turbulence, which is characterised by its chaotic nature, and is therefore complicated to model rigorously at a mathematical level: for this reason, the Reynolds-Average Navier Stokes (RANS) equations are introduced. This technique makes it possible to apply the Reynolds decomposition to the Navier-Stokes equations (1), filtering out the chaotic turbulence: this allows to decouple the steady state flow from the time-dependent fluctuations, that are treated by a separate model that we discuss in the following paragraph (2.1).

2.1 Turbulence model[1]

Using RANS equations, we numerically calculate the average velocity of the flow field. However, for smaller time and space scales, we use modeling techniques. As a result, RANS calculations are very efficient in terms of computational performance, but they can be greatly affected by the selection of turbulence models. Two-equation turbulence models utilize the resolution of two distinct transport equations to determine both a turbulent length and time scale. The *Standard $k - \varepsilon$ Model* is a commonly used model in engineering flow calculations, which is based on transport equations for turbulence kinetic energy (k) and its dissipation rate (ϵ). However, in this study we have chosen to implement the *Realizable $k - \varepsilon$ Model*, which is an updated version of the Standard model and includes improvements. Specifically, it includes a revised formulation for turbulent viscosity and a modified transport equation for the dissipation rate (ε) that was derived from an equation for the transport of mean-square vorticity fluctuations. The term "realizable" refers to the fact that this model is consistent with the physics of turbulent flows. The modeled transport equations for k and ε in the Realizable $k - \varepsilon$ model are:

$$\frac{\partial}{\partial t}(\rho k) + \frac{\partial}{\partial x_j}(\rho k u_j) = \frac{\partial}{\partial x_j}\left[\left(\mu + \frac{\mu_t}{\sigma_k}\right)\frac{\partial k}{\partial x_j}\right] + G_k + G_b - \rho\varepsilon - Y_M + S_k \tag{2}$$

$$\frac{\partial}{\partial t}(\rho\varepsilon) + \frac{\partial}{\partial x_j}(\rho\varepsilon u_j) = \frac{\partial}{\partial x_j}\left[\left(\mu + \frac{\mu_t}{\sigma_\varepsilon}\right)\frac{\partial \varepsilon}{\partial x_j}\right] + \rho C_1 S\varepsilon - \rho C_2\frac{\varepsilon^2}{k + \sqrt{v\varepsilon}} + C_{1\varepsilon}\frac{\varepsilon}{k}C_{3\varepsilon}G_b + S_\varepsilon \tag{3}$$

In these equations, μ_t is the turbulent (eddy) viscosity and is obtained as $\mu_t = \rho C_\mu\frac{k^2}{\varepsilon}$, where C_μ is no longer a constant, being a function of the mean strain, the rotation rates, the angular velocity of the system rotation and the turbulence fields k and ε. G_k represents the generation of turbulence kinetic energy due to the mean velocity gradients, G_b represents the generation of turbulence kinetic energy due to buoyancy, Y_M represents the contribution of the fluctuating dilatation in compressible turbulence to the overall dissipation rate, $C_{1\epsilon} = 1.44$ and $C_2 = 1.9$ are constants, $\sigma_k = 1.0$ and $\sigma_\epsilon = 1.2$ are the turbulent Prandtl numbers for k and ϵ, S_k and S_ϵ are user-defined source terms. Moreover $C_1 = \max\left[0.43, \frac{\eta}{\eta+5}\right], \eta = S\frac{k}{\varepsilon}, S = \sqrt{2S_{ij}S_{ij}}$

2.2 Pollutant Transport Equations[2]

When using ANSYS Fluent to solve the conservation equations for chemical species, the local mass fraction of each species (Y_i) is predicted by solving a convection-diffusion equation for the ith species. The general form of this conservation equation is as follows:

$$\frac{\partial}{\partial t}(\rho Y_i) + \nabla \cdot (\rho \mathbf{v} Y_i) = -\nabla \cdot \mathbf{J}_i + R_i + S_i$$

The net rate at which a specific species is produced by chemical reactions is represented by R_i, and the rate at which that species is generated from the dispersed phase or from any specified sources is represented by S_i. In turbulent flows, the mass diffusion $\mathbf{J}_i$ has the following form:

$$\mathbf{J}_i = -\left(\rho D_{m,i} + D_t\right)\nabla Y_i - D_{T,i}\frac{\nabla T}{T}$$

---

[1]Ansys Fluent Theory Guide, 15317, ANSYS Inc, USA (2013), pp. 47-55
[2]Ansys Fluent Theory Guide, 15317, ANSYS Inc, USA (2013), pp. 187-188

where $D_{m,i}$ and $D_{T,i}$ are respectively the mass diffusion coefficient and the thermal diffusion coefficient for the ith species in the mixture and D_t is the turbulent diffusivity. In our study the last term in neglected since $\nabla T = 0$.

It is important to note that, given the desire to study the concentration of a pollutant transported by a flow, it is assumed that the former itself does not modify the characteristics of the latter: the percentage of pollutant in the air is in fact sufficiently limited to satisfy this assumption.

2.3 Boundary conditions

The conditions at the boundaries of a system are a fundamental component: they ensure that the system has a mathematical solution. However, boundary conditions are not only important for the mere numerical resolution of the equations being studied; they are also fundamental data that reflect and encode situations that arise in the more practical aspects of a study. In this section we present our choices in this regard.

2.3.1 Velocity Inlet

In computational fluid dynamics (CFD), inlet velocity boundary conditions are used to specify the flow characteristics at the inlet of a system or computational domain. One way to specify an inlet velocity boundary condition is to use a constant velocity profile, in which the velocity of the fluid remains the same throughout the inlet cross section: this is the setting we choose to be the most likely for the study, setting an inlet velocity of $5m/s$.

2.3.2 Pressure Outlet

When the inlet condition consists of a flow velocity rate, it is a common procedure to use a pressure outlet boundary condition, which fixes the pressure and sets the velocity gradient to 0. This decision comes from the fact that le domain is set sufficiently long to allow the flow to reach the fully developed state, where there is no change in the flow direction. In these simulations, the excess pressure with respect to the atmospheric pressure is set to the default value of 0.

2.3.3 Symmetry

A symmetry boundary condition is applied at the top of the domain, causing the developed flow field pattern to be reflected along this boundary. This boundary condition imposes no flow or scalar flux across the boundary, which is consistent with the realistic behavior of the flow in this situation.

2.3.4 Walls

The buildings, ground and chimney are the only solid surfaces in the simulation. Since air cannot pass through these surfaces nor slide over them, a no-slip condition is applied to these surfaces.

3 Baseline case

As a starting point, we consider a simplified scenario with respect to what will be the actual study of interest. This preliminary step allows us to more effectively and rigorously define the geometry of the problem, the numerical discretization of the domain, and the correctness of the implemented models, also from a physical likelihood point of view. Therefore, we consider a domain analogous to the one briefly described in the introduction consisting of a side view of a longilinear building and a nearly point source of pollutant placed "on top" of another building upstream of the flow. For this initial problem we will conduct simulations designed to verify that the constitutive assumptions of the design are correct and consistent.

3.1 Geometry setup

The domain under consideration consists of a rectangle of height $40m$ and length $120m$, from which we "cut out" a rectangular shape representing a building of height $9m$ and length $3m$. The size of the domain was set a posteriori in order to represent the whole flow of interest. Please note that the dimensions considered do not wish to be completely realistic, but only to reproduce plausible proportions and values: this allows not to compromise the physical veracity of the model while keeping the computational cost affordable. The flow of the simulated fluid occurs from left to right: in the following we identify the left side as inlet and the right side as outlet. The pollutant source is placed at a height of $5m$ along the left edge of the domain, and is represented in the geometry by a fraction of this side of length $0.5m$. Furthermore, assuming that the pollutant is emitted from an additional construction (e.g. a chimney), below this source the inlet edge represents a wall of the latter. This last choice deserves further investigation from a modeling point of view. Before arriving at this setup, we simulated the problem with a point source "suspended" between two flow inlet zones. However, by doing so, the pollutant flowed above the buildings without interacting with them, being carried at high speed by the laminar inlet flow. Given the limited interest in studying this scenario, we attempted to replicate more realistic circumstances, and for this we updated the setup as reported above. In any simulation conducted in this, given the presence of an inlet flow only above the source, it is immediate to observe a recirculation zone adjacent to the chimney. We therefore investigate whether this behavior is justified from a physical point of view. We verify that placing the chimney at the inlet is equivalent to representing a laminar flow over the entire inlet with a chimney downstream of it.

3.2 Mesh

To study this scenario, we implemented numerous grids before finding the best solution. Given the size of the domain and the complexity of the problem, it is in fact necessary to investigate which type of discretization allows to find solutions with the smallest possible errors while containing the computational efforts required. In order to achieve this important result, we followed the following steps.

First, looking at the geometry of the problem, it is evident that the choice of a uniform mesh is not the best possible solution. In fact, if it is in our interest to have an approximation as accurate as possible of what happens near the walls and, in particular, in proximity of the building. At the same time it is not as relevant to have an accurate definition in regions of space not strictly related to to our case study. Furthermore, it is evident that in the nearest of the walls there will be the greatest difficulties, since in these regions the fluid comes into contact with the imposition of the boundary condition (specifically, the no slip condition). For this reason it is wise to implement a non-uniform mesh. To do this, the 'inflation' feature was exploited. Inflation allows us to change the mesh size as we approach the considered boundaries. In our case, it has been imposed to the edges at the base of our geometry. More specifically, the total thickness option was chosen and the number of layers was set at 30, with a growth rate of 1.05. This solution allowed us to obtain respectable mesh quality results, but drastically increased the number of elements in the nearest of the zones of interest. In particular the growth rate value was carefully chosen, as a higher value would have resulted in more irregular elements and thus poorer overall quality.

One problem that may arise as a result of this process is the creation of excessively irregular elements. To verify that the mesh obtained has an acceptable quality, it was decided to check certain parameters, including, in particular, skewness and orthogonal quality. Skewness is defined as the difference between the shape of the cell and the shape of an equilateral cell of equivalent volume, while orthogonal quality is related to how close the angles between adjacent element faces (or adjacent element edges) are to some optimal angle.

After defining the parameters to be checked, a grid independence study was implemented to decide which mesh to use. The idea is to compare increasingly refined meshes until a configuration is found after which no more significant changes or particular anomalies are observed in the solutions. Thus, starting with very coarse meshes, the rate of discretization is increased until one is sufficiently sure of the final

quality. Therefore, the grid independence study was carried out. Starting with very loose meshes, an optimal discretization was achieved to simulate the problem.

To simulate the problem, the number of iterations is set each time to a value which attains a plateau in the plot of the residuals.

It has been possible to observe that, considering a very loose mesh, the solution is not reliable. This can be seen very easily by looking at the residue graph, which shows non-negligible jumps over the 800 iterations considered. This fact is better shown in figure 1. By gradually increasing the number of
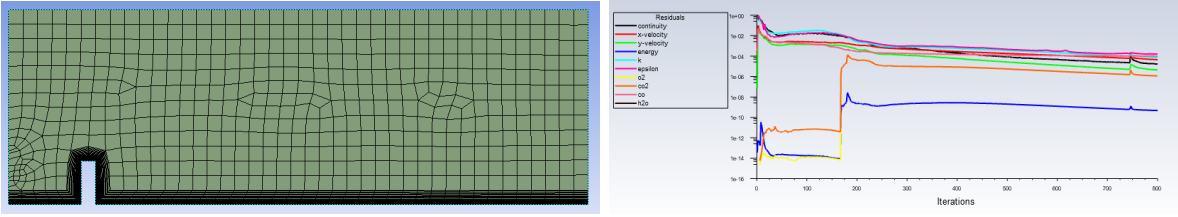
Figure 1: Coarse mesh and residuals plot

elements that make up the mesh, an overall improvement in performance can be seen. In particular, this can be stated not only from the graph of residuals (which shows a continuous and steady decrease in their value), but also from the fact that roughly constant values are achieved in the problem-defining variables. For example, looking at figure 2, it can be seen that a loose mesh fails to fully capture the velocity trend, which is instead well defined with more refined meshes.
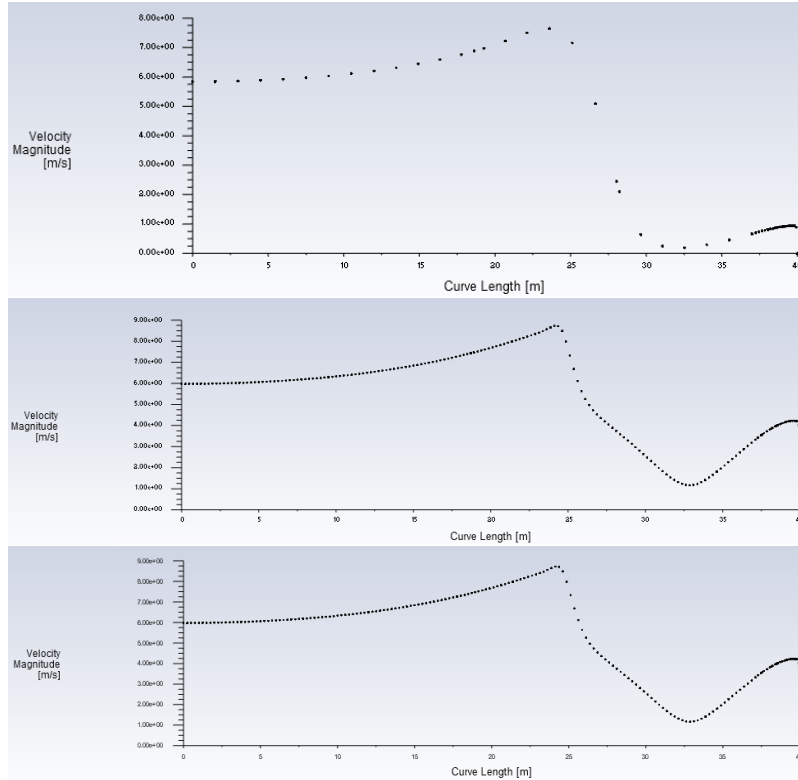

Figure 2: Velocity magnitude profile at $x = 30m$ for elements of edge $1.5m$, $1m$ and $0.25m$

Therefore, a mesh with elements of side $0.25m$ was chosen, which leads to not excessive computational cost, acceptable worse skewness and orthogonal quality and, at the same time, good quality solutions. The mesh considered can be observed in figure 3. More precisely, our mesh has 82507 nodes and 81827
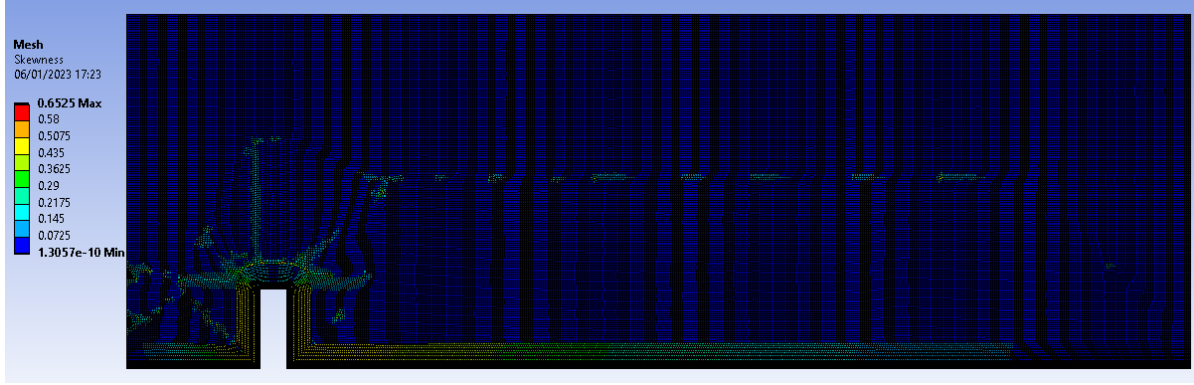
elements.

Figure 3: Skewness for the chosen mesh

3.3 Fluent simulation

3.3.1 Materials

As mentioned above, it was decided to simulate the effects of a pollutant in the air. To this end, the 'species' section within the software was modified in order to be able to change the composition of the air and insert carbon monoxide (specifically, 0.01% of the total air mass). This substance is released from the chimney located in the inlet. To do this, a source section was inserted. Specifically, two different heights were tested, as discussed later on.

3.3.2 Boundary condition

Following the section 2.3, appropriate boundary conditions must be imposed to solve the problem. Specifically, an inlet velocity of $5m/s$ was imposed. In addition, the lower portion of the input side of the domain was bound to a wall condition, in order to simulate the presence of a chimney, which ends with the mouth of the chimney that generates the pollutant. At this point the "source" region is therefore inserted, in which the presence of carbon monoxide is imposed.

3.4 Results

To solve the problem, a SIMPLE scheme was used, while for spatial discretization, a second order upwind was chosen. In this section, we briefly report the results for the first scenario. We can see that the results
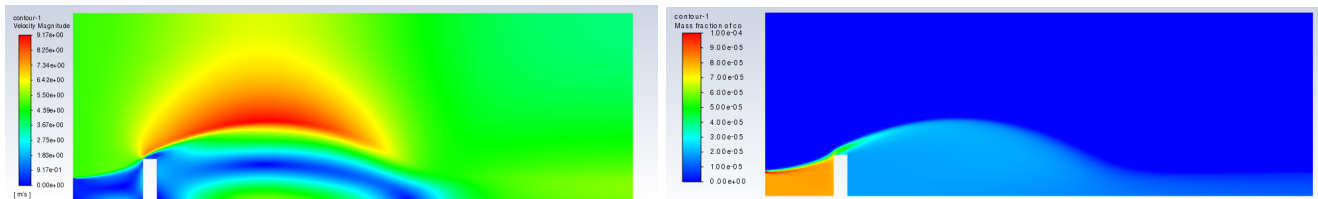

Figure 4: Velocity magnitude (left) and CO mass fraction (right) for lower source

are perfectly consistent with practical experience. This is a further indicator of how suitable the mesh is for our purposes. Furthermore, the goodness of the chosen geometry can be highlighted by showing how each value assumed by the flow velocity is largely contained within the simulated region, thus avoiding possible inconsistencies due to the encounter with a boundary condition. As far as the phenomenon in

question is concerned, we are able to observe the behaviour of the velocity of the incoming air flow, which is affected by the presence of the building, creating a recirculation region both behind and in front of it. This effect is then reflected in the distribution of the pollutant, which appears to follow a similar path. It is worth noticing, how a portion of this tends to concentrate on the face of the building. This kind of behaviour highlights the usefulness of the study.

4   Two buildings case

At this point, we extend the baseline case to consider functional scenarios for our study. We introduce a second building into the geometry of the problem, identical to the first one already described and positioned behind it. Let us consider variations obtained by placing the two buildings at a distance of 10m and 20m, again differentiating the cases where the pollutant source is placed at two different heights from the ground (5m and 11m). We intend to study how in the different cases a first structure can act in shielding the space behind it.

The dimensions of the domain have already been set large enough (120m) to ensure the correct simulation of the flow even after this addition, especially with regard to the total length of the section considered. In any case, it will be necessary to verify the correct choice of this distance by analysing a posteriori that the simulations obtained represent the phenomenon in its entirety, without negative interactions with the outlet conditions.

As far as the mesh is concerned, the same inflation already detailed is applied to the edges of the new construction, in order to allow for refinement near the walls, where we expect rapid variations in the variables.

In order to assess the pollution received by the second building in the different scenarios, it is necessary to find a scalar quantity that is related to the amount of carbon monoxide that hits the wall facing the inlet. To this end, we calculate the integral average of the mass fraction of CO along the facade considered as

$$\frac{\int_\Gamma mf_{CO}}{|\Gamma|}$$

where Γ is the rectilinear wall considered. This value is not compared to a reference number, but only compared between different cases, so as to assess the variations obtained. Each result obtained will be accompanied and motivated by the simulation of the entire flow in the domain.

4.1   Results

First, let us analyse the velocity magnitude plots for the 4 cases of interest (Figure 5). It is evident that the location of the pollutant source has a great impact on the solution, while the distance between the two buildings only seems to slightly affect the size of the affected zones. The passage of the flow above the obstacles generates lower velocity zones behind them, of varying magnitude depending on the parameters of the geometry. These are recirculation zones of the flow, as also evidenced by the vector plots in Figure 6, where due to the upstream presence of the buildings the flow takes on a considerable vorticity. The contact with walls and terrain also slows the flow velocity as a consequence of the imposed no slip condition. However, the most pronounced difference lies in the fact that when the source is at a lower height than the buildings, the flow is significantly accelerated above the first obstacle, with peak velocities of $8m/s$, far greater than the velocities obtained in the case where the source overhangs the two buildings.

Given the considerations just made, we expect to observe very different concentrations of the pollutant depending on the given chimney, since as shown in Section 2.2, the transport and diffusion of the monoxide depend on the velocity and pressure field of the airflow. Firstly, we note that the pollutant mass is non-negligible in most of the lower section of the domain, if not very far from the inlet. A high fraction of
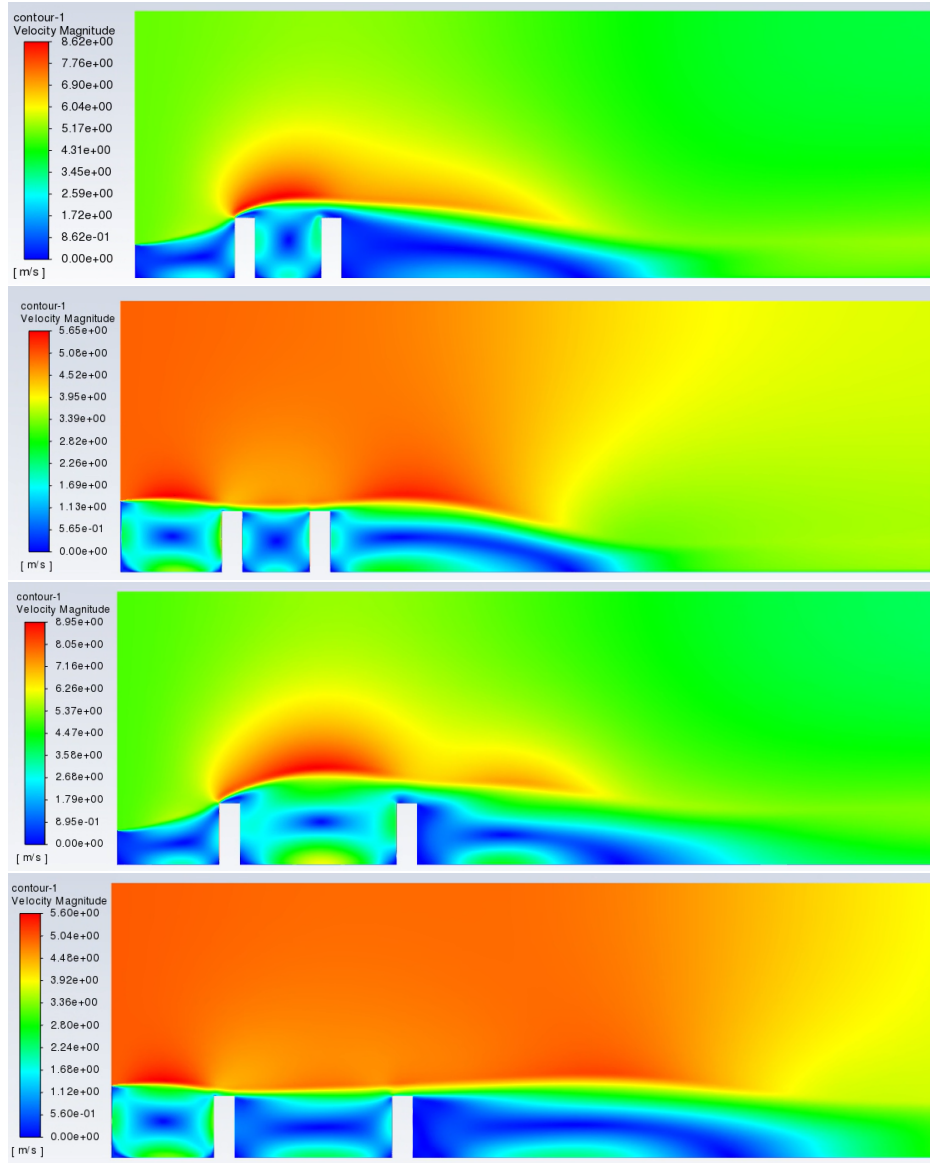
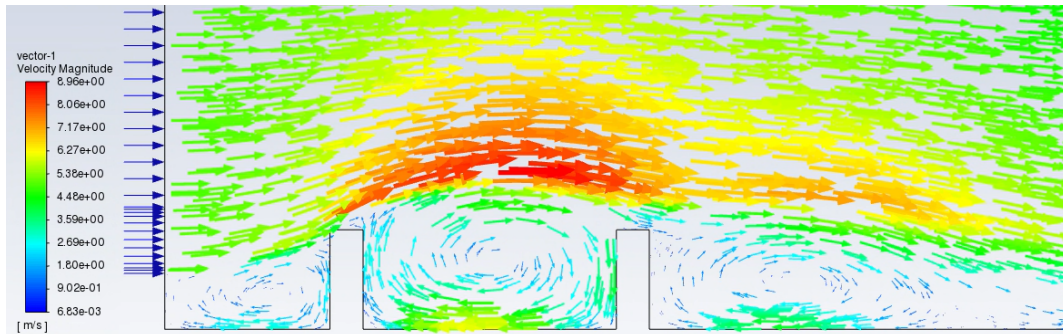Figure 5: Velocity magnitude (different scales) in the 4 cases considered

Figure 6: Example of velocity vector plot

the pollutant remains 'trapped' by the initial recirculation downstream of the chimney. In a natural way, pollution is at its highest near the source, which is also accentuated by the presence of the first building

that creates the large area in question. However, in all four scenarios constructed, the pollutant flow is not completely screened by the first barrier present, but continues downstream, albeit with much lower concentrations. The difference in pollutant behaviour will be investigated in the next section in a more accurate and quantitative manner. On a final remark, we point out how the second building once again acts as a screen to the downstream part of the domain and to other eventual objects.
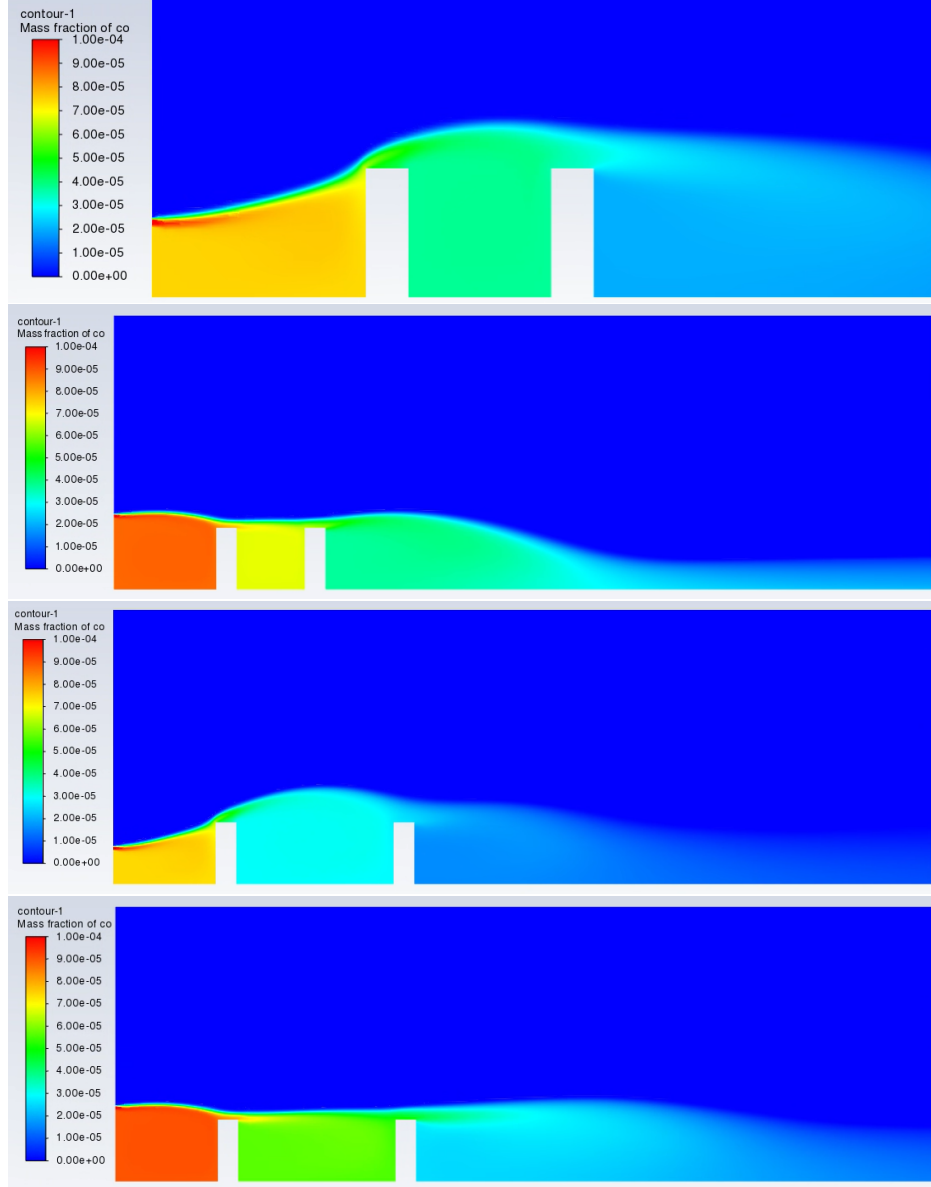

Figure 7: CO mass fraction (different scales) in the 4 cases considered

5   Final considerations

Table 1 shows the results obtained for the integral average of the mass fraction of CO in the flowing air along the segments that make up the upstream walls of the buildings. The mass fraction in the inlet flow from the source was set to 0.01%. However, the results are difficult to evaluate as an absolute measure. Hence, these values offer a relative measure of the pollution reaching these areas which is comparable for all scenarios.

	Lower source			Higher source		
	Single	10m dist	20m dist	Single	10m dist	20m dist
Front build.	0.0079%	0.0074%	0.0072%	0.0086%	0.0087%	0.0089%
Back build.	-	0.0039%	0.0029%	-	0.0067%	0.0055%

Table 1: Average mass fraction of CO on facades

Firstly, we observe that the value for the first building slightly varies when distinguishing the cases with the two different sources. Due to the higher chimney present at the inlet, a greater recirculation happens in the latter case, carrying more pollutant towards the facade of the first structure. However, this is substantially independent of the number of buildings and the distance between them. The flow downstream of the building only slightly influences the flow near the entrance, so the result is plausible. However, the most relevant results for our scope are those for the second structure. As expected from our initial problem, these values vary significantly between the four different contexts reported.

Firstly, a lower source seems to cause less pollution. This result is not surprising: it is indeed plausible that a source lower than the first obstacle, in the absence of substantial buoyancy of pollutant particles, is largely shielded from it. As already noted, this obstruction is not total, mainly due to the strong turbulence of the flow above the obstacle, which carries the pollutant further downstream at high speed.

Secondly, the internal distance also seems to influence the values, albeit more slightly. A smaller distance causes a higher level of pollution according to our parameter. This proves that a closer building is not necessarily better shielded from the pollution; on the contrary the narrower section in between the opposite walls, which could represent a street, is more affected in this scenario. This happens in the same way regardless of the height of the source.

6   Conclusion and future developments

The study conducted above indicates that a preliminary analysis during the design of new urban areas can significantly impact the pollution received by buildings (and consequently their windows) and internal roads.

We can suggest some precautions:

- A first 'boundary' building between the chimney and the city, if higher than the former, significantly reduces pollution of the areas behind it. However, it must be considered that in this way a high concentration of pollutant remains in circulation in the vicinity of the source, with no possibility of dispersion under the conditions examined.

- Narrow internal roads (also known as 'street canyons') near city boundaries may suffer from heavy pollution. It is therefore advisable to avoid sensitive buildings in areas with these characteristics, or to design streets of greater width in the suburbs.

- Two consecutive buildings can screen the areas behind them significantly better than a single obstacle, generating an 'inner' area in which the pollutant is trapped.

All in all, the pollution of the second building in the best case studied is almost half of that of the worst case, proving that the proposed strategies can be highly effective, more so if optimized. The results obtained for the optimal design of an urban agglomeration can likely be extended to further cases through the definition of more complex geometries in the future, providing a powerful tool for urban planners to minimize pollution levels in new urban areas.